ON THE DURATION OF LOW SPEED DYNAMIC STALL

by

R.A.McD. Galbraith
A.J. Niven
+L.Y. Seto

University of Glasgow,
Scotland.

+ British Marine Technology,
London, England.

Abstract

The paper considers dynamic stall of aerofoils and, in particular, the duration of the stall once it has been initiated. The stalling process is likened to a transition from a streamlined flow to that of a bluff body where the flow development is governed by the mean flow. It is concluded that the present data favours this transition occurring soon after stall onset and, because of this, there are constant non-dimensional time delays associated with the process; independent of reduced frequency/pitch rate and aerofoil shape etc.

Nomenclature

C	chord length (m)
k	reduced frequency ($\omega c/2V$)
k_1	reduced pitch rate ($\dot{\alpha}c/2V$)
t	time (s)
V	free stream velocity (m/s)
α	angle of attack (degs)
$\dot{\alpha}$	pitch rate (rad/s)
τ	non-dimensional time delay ($\Delta tV/c$)
ω	frequency (rad/s)

I. Introduction

The search for an acceptable quantitative description of dynamic stall has been difficult and, although good progress has been made[1,2,3,4], much remains unknown or confused[5,6]. Each contribution to the understanding of the phenomenon is particularly useful for the assessment of rotor dynamic aircraft performance limits. In general, dynamic stall may occur on any aerofoil whose effective incidence varies significantly with time. In particular, at the high speed boundary of a conventional helicopter's flight envelope, the retreating blade is susceptible to dynamic stall due to the imposed cyclic pitch necessary for proper trim requirements. From the empirical data that have been collected (eg, ref. 7) a generally accepted qualitative description of the phenomenon has evolved and is as illustrated in fig. 1 and tab. 1[8]. An explanation of the distinctive aerodynamic loadings observed involves the division of the process into four distinct phases of flow development. Of particular relevance to this paper, are the two phases of vortex movement and full stall development which may be considered as a transition from streamlined flow to that termed bluff. There is some confusion as to the precise timing of this transition and it is hoped that the present paper will contribute to its alleviation

The build-up and subsequent passage of the "dynamic-stall vortex" produces a distinctive pressure wave over the aerofoil. This has been presented using both psuedo three-dimensional plots

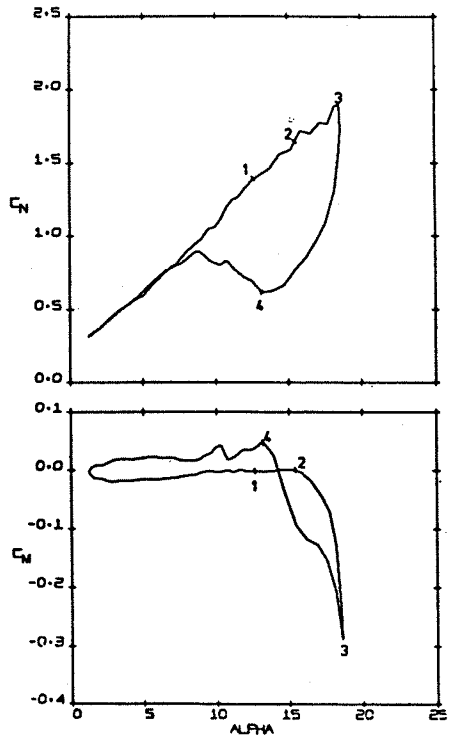

Fig. 1. DYNAMIC STALL EVENTS

	FORCES AND MOMENTS
1	EXCEEDS STATIC MAXIMUM LIFT. EXTRAPOLATE LINEAR RANGE.
2	PITCHING MOMENT DIVERGENCE. VORTEX LIFT PRESENT.
3	MAXIMUM LIFT, RAPID DECAY. MAXIMUM PITCHING MOMENT.
4	READJUST TO LINEAR RANGE.

	FLOW STRUCTURE
1	FLOW REVERSALS WITHIN BOUNDARY LAYER. FORMATION OF VORTEX
2	VORTEX DETACHES AND MOVES OVER AIRFOIL SURFACE.
3	VORTEX PASSES TRAILING EDGE. FULL STALL DEVELOPS.
4	REATTACHMENT OF FLOW.

TABLE 1. FLOW STRUCTURE.

and surface contours of pressure time histories[9]. From direct graphical observation of these contours, Carta found the wave velocity and, hence, stall development, to be dependent on the model motion, and in particular the reduced frequency (see fig. 2).

SYMBOL	AIRFOIL	M	f	α_M	$\bar{\alpha}$	REF (FIG.)
○	VERTOL 13006 – 0.7	0.2	24	12	5	11(24)
□	VERTOL 13006 – 0.7	0.2	48	12.5	5	12(12)
△	VERTOL 13006 – 0.7	0.3	12	10	5	11(20)
◇	VERTOL 13006 – 0.7	0.3	68	10	5	11(22)
D	VERTOL 13006 – 0.7	0.4	48	10	5	11(25)
◖	VERTOL 23010 – 1.58	0.4	94.3	12.5	5.7	10(33)
●	NACA 0012	0.4	89.3	12.2	5.9	10(40)
■	NACA 0006	0.2	12	7.5	5	12(6)
▲	NACA 0006	0.4	48	10	5	12(11)
◆	NACA 0006	0.6	72	10	5	12(10)
◖	NACA 0012	≈0.1	≈1	15	14	9

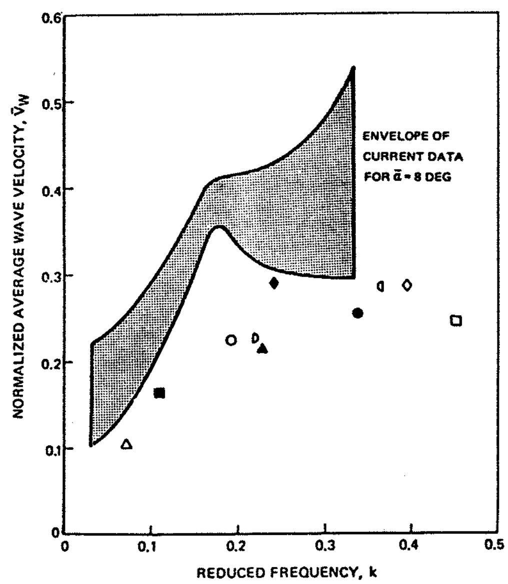

Fig. 2. WAVE VELOCITY COMPARISONS (Ref. 9)

Extensive flow visualisation tests were carried out by Robinson[10] and his data, like that of Carta's, showed a dependency of the vortex velocity with reduced frequency (fig. 3). In addition, the data presented illustrates little dependence of vortex travel on Reynolds number for the limited test range presented.

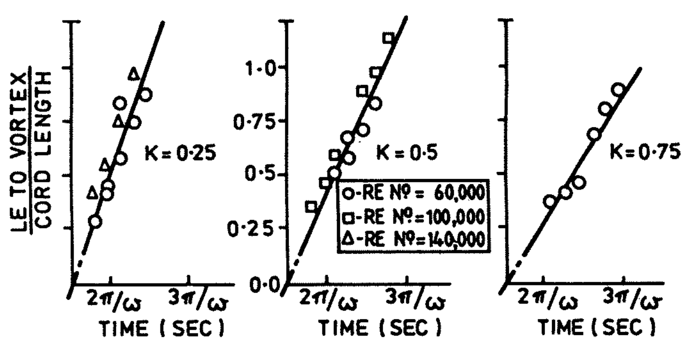

Fig. 3. VORTEX CENTER LOCATION (REF. 10)

The passage of the vortex over the aerofoil surface manifests itself in the aerodynamic loadings, and so the time histories of the appropriate coefficients may be used as an indicator of average development time. Aihara et al[11], in some unusual experiments, observed that, for low Reynolds numbers, there was a clear dependency of vortex velocity on reduced pitch rate. His result has been re-drawn in fig. 4 where the abscissa is a non-dimensional rise time which is proportional to both rise angle and the inverse of the reduced pitch rate.

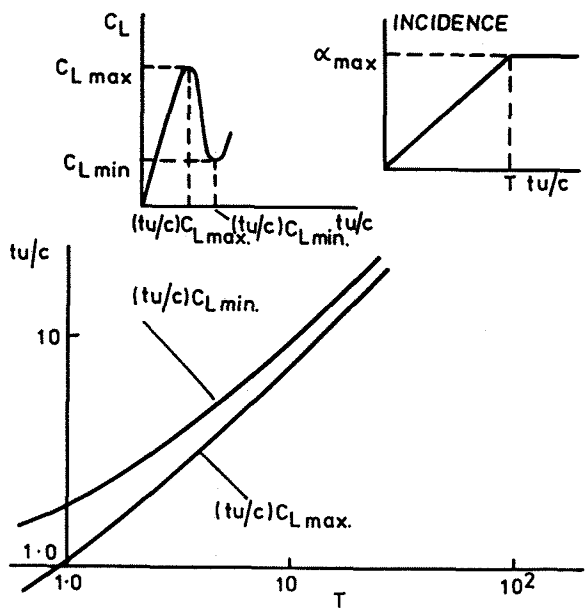

Fig. 4. EXPERIMENTAL RESULTS OBTAINED BY AIHARA ET AL (REF. 11)

When considering a practical method for the prediction of unsteady aerodynamic loadings for helicopter rotors, Beddoes[12] adopted a statistical analysis of some 300 specific test cases exhibiting similar dynamic stall characteristics. The analysis incorporated integrated pressure data and Beddoes concluded that, to a first order, there was a common time scale associated with the stall events; a typical non-dimensional time difference is illustrated in fig. 5. The most interesting conclusion to follow from this analysis was, that the time delays appeared to be independent of reduced frequency, model motion and aerofoil shape etc.

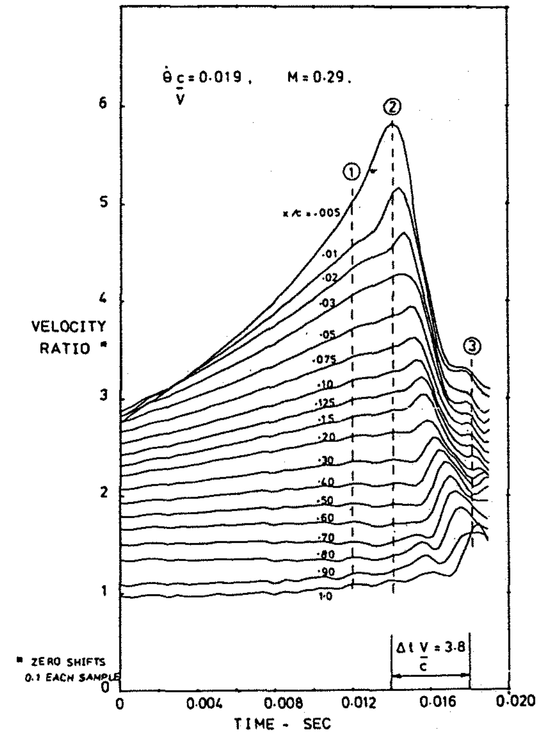

Fig. 5. DYNAMIC STALL - CHORDWISE PROGRESSION

Recently, Galbraith and Seto[13], whilst assessing the limitations of their test facility for ramp motions, observed that the data implied a constancy of time delay between stall onset and the passage of the vortex from the trailing edge. The stall development was therefore independent of the model pitch rate and this was used to extend their test range. The data, illustrated in figure 6, was obtained by isolating two well defined timing marks on particular chordal pressure histories. Stall onset was assumed to have had occurred when the pressure coefficient at the 34% chord diverged, and the stall vortex was assumed to have passed the trailing edge when the pressure coefficient peaked at the 97% chord location.

There is, therefore, some variance between the respective works. Such differences may, in part, be due to the variety of analysis used, data considered and to the lack of a unique method of determining the event timing of vortex initiation and full stall development. This very problem also

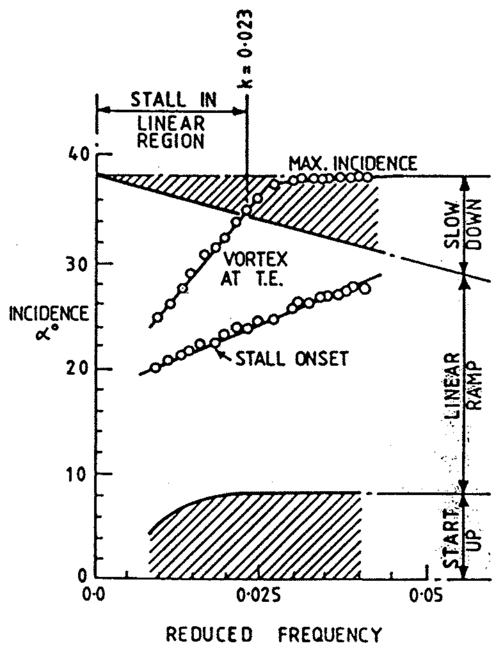

$\left[k \equiv \frac{\dot{\alpha} c}{2V}\right]$

Fig.6. LIMITS TO THE EXPERIMENTS

afflicts the present work, but for each aerofoil and each data set, consistent discriminators have been used. On the basis of the data to be presented, it has been concluded that, once stall is initiated, the subsequent development is decoupled from the model and model motion, ie, it is free-stream dependent and, as such, more akin to bluff body flow than that over a streamlined shape.

II. General Discussion

When an aerofoil transits from a steamlined flow to the fully stalled condition, it, in effect, becomes a bluff body. Under dynamic conditions, this implies that the flow changes from a dependency on the aerofoil state to that of free stream, where the associated wake will be insensitive to the detailed aerofoil shape.

It may not, however, be independent of model motion, for it is well known that vortex induced oscillations of long undamped slender cylinders exhibit a "lock in" effect where both the wake and the body motion reinforce each other. At first thought therefore, one may expect that the stall development of an oscillating aerofoil would not coincide with that subjected to ramp like motions. Further, comparing oscillatory data with that from ramp like motions will be complicated by the oscillatory aerofoil moving both in and out of stall.

In contrast to this, one may assume that dynamic stall development is governed by a basic common process and, therefore, similar observations for different motions can be made. The process may, thus, be simplified if the stall development were decoupled from the model motion at an early stage. In particular, if the stall development were freestream dependent shortly after initiation. There should then be a comparability of development for all model motions.

The data to be presented and arguments developed all relate to the development of the stall once stall onset has occurred. For the present work, the manner of the initiation is only relevant, in as much as it affects the timing of stall onset. Most of the data to be presented have been taken from the Glasgow University data set which contains data for a NACA 23012 section and a modified version with a reflex trailing edge designated 23012A. The collection and cataloguing of the data is described in refs. 14, 15, 16 and 17.

Glasgow University Data

Typical data from the Glasgow University facility are presented in fig. 7. The pressure wave, normally associated with vortex travel, is clearly illustrated on both the contour plots and the three-dimensional representation of the pressure histories. The gross effect this has on the overall lift and pitching moment coefficients is also clearly illustrated and it may be seen that whilst the C_N dynamic overshoot is large, the modification to the pitching moment is greater.

It is from data such as these that one can assess the non-dimensional time delays associated with the stalling process. The average normalised wave velocity[9], taken as representing the rate of

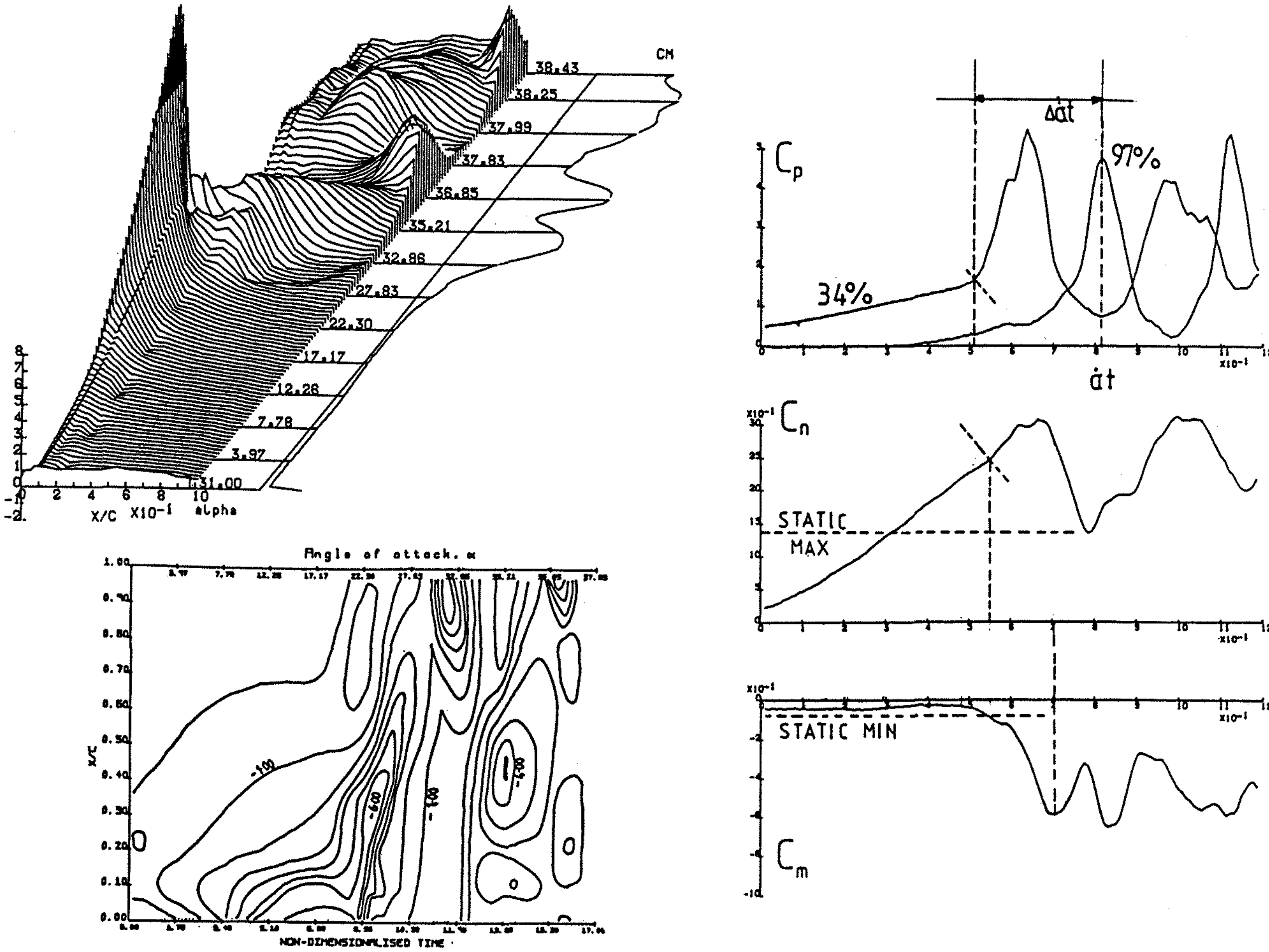

Fig. 7. STANDARD PRESENTATION FOR GLASGOW UNIVERSITY DATA
Shown above: NACA 23012, $Re = 1{\cdot}5 \times 10^6$, $k_1 = 0{\cdot}035$

stall development, may be assessed from the contour plots, but the large gradients to be measured and uncertainties involved would probably result in much scatter of the data. Wherever possible, the authors have used an alternative method in which the time between two well defined events on the upper surface pressure history of the aerofoil is taken to represent stall development.

From the three-dimensional representation of the upper surface pressure, it may be observed that there is an unmistakable peak in the trailing edge pressure distribution and this, as discussed in ref. 13, is taken to be the point at which the vortex breaks away from the trailing edge and there is a subsequent in-rush of fluid to the low pressure region. This peak was assumed to be representative of stall completion. To indicate that stall had been initiated, the divergence of the 34% chord pressure history, was chosen. The time delay associated with these two discriminatory points is as indicated on fig. 7. As will be discussed later, the first of these timing points is highly dependent on the model itself and hence the manner of stall onset.

Where it was inappropriate to use the individual surface pressure histories, the overall C_N and C_M and C_D characteristics have been used. This was done for both the low Reynolds number data, where signal to noise ratio deteriorated, and when considering data from ref. 7.

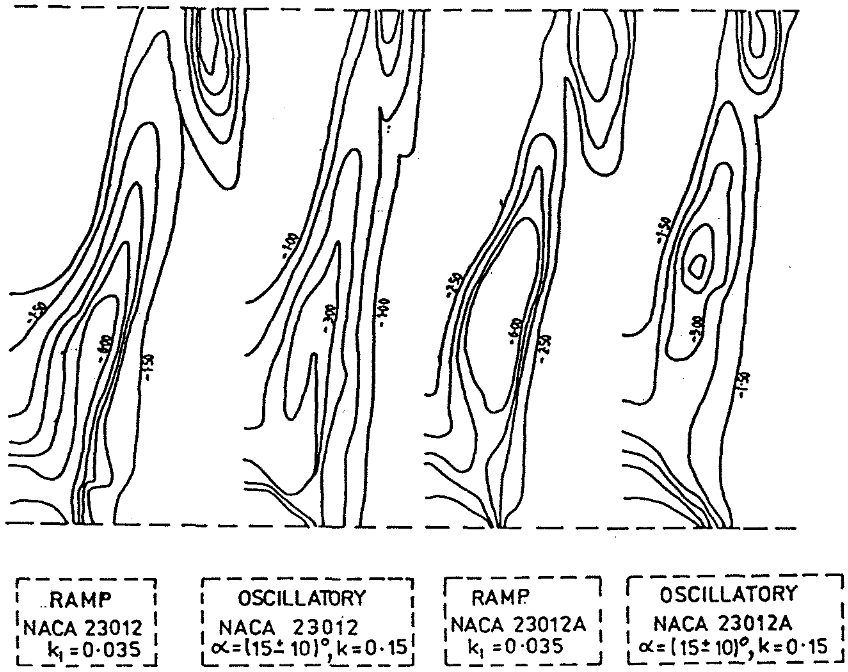

Fig.8. CONTOUR PLOTS for VARIOUS TEST CASES

Deep Stall Development

When the pressure wave or ridge that travels down the aerofoil during dynamic stall is isolated from the contour plots and selected runs compared, see fig. 8, one can observe that the gross features of the process, are common for the data presented. Apart from the very obvious ridge there is a secondary wave, which penetrates a short distance up the chord from the trailing edge. It is the peak on this secondary ridge that provides the terminal timing mark for stall development discussed above. It would be difficult to distinguish between these four contour plots purely on the basis of reduced frequency or model motion etc, for their relative inclination is small, albeit the wave strengths vary and peak at different chordal locations. It will be noted from fig. 8, that two models and model motions have been considered. The Reynolds number, however, was constant at 1.5 million, and the associated Mach number was approximately 0.11.

The contour plots, whilst most interesting, are of limited quantitative value, in that the assessment of wave velocities would be subjective and prone to errors caused by the graphical assessments of large, ill-defined gradients. Both the degree of subjectivity and inaccuracy may be reduced by the use of the two well defined discriminatory events of the stall, as mentioned earlier. From these, we can obtain a consistent timing of stall development and for the pitching motions considered, the associated non-dimensional time delays are:

$$\text{Ramp delay} = \tau_r = \Delta(\dot{\alpha}t)/2k_1 \qquad (1)$$

$$\text{Sinusoidal delay} = \tau_s = \Delta(\omega t)/2k \qquad (2)$$

The data that follows from the two aerofoils contained in the current Glasgow data set are illustrated in fig. 9 where $\Delta(\omega t)$ and $\Delta(\dot{\alpha}t)$ are plotted against 2k and $2k_1$ respectively. From the above equations (ie 1 and 2) a straight line on these figures indicates a constant time delay independent of reduced pitch rate/frequency. Whilst well correlated straight lines were obtained for each model for both ramp and oscillatory conditions, there is a small difference between their respective gradients.

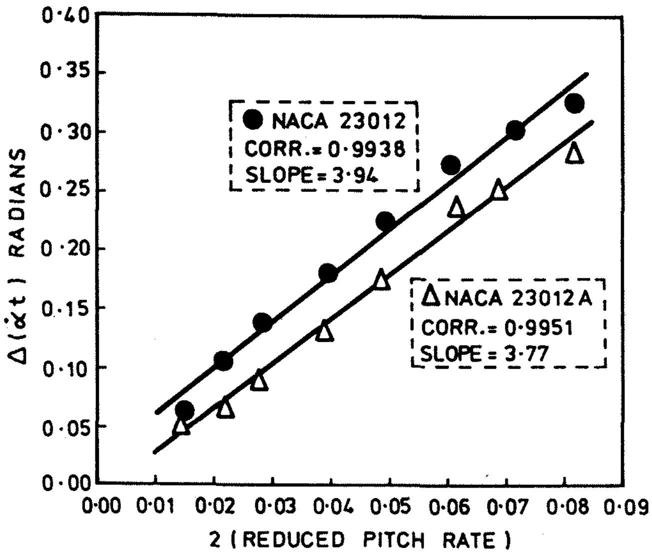

Fig. 9(a). TIME DELAY PLOT-RAMP

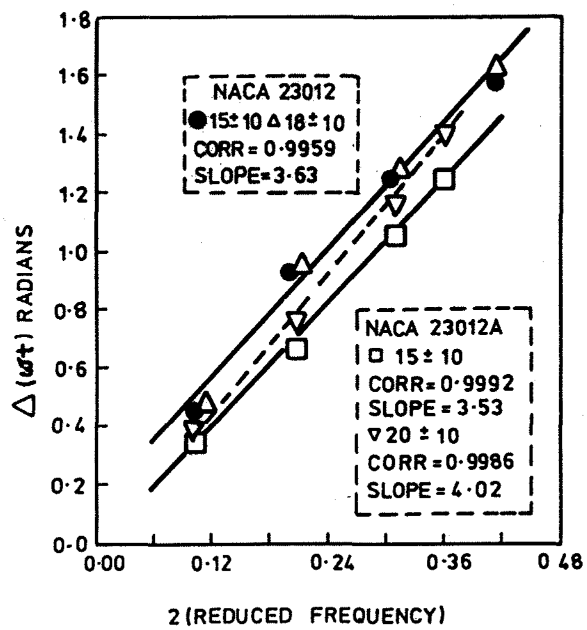

Fig. 9.(b) TIME DELAY PLOT-SINUSOIDAL

It is thought that this difference is a consequence of the manner in which the initial timing mark, indicating that stall has occurred, is inconsistent between models. This is illustrated in fig. 10 where pressure histories at 34% and 97% chord are presented. These are typical histories and it may be observed that, the behaviour of those at 34% chord are different in the region of stall onset. The two criteria used for the models are as indicated and it is clear that, for the unmodified NACA 23012, the stall onset, as we have defined it, occurs before the comparable definition on the modified version and in a different manner. It is to be expected, therefore, that for ramp motions, the time delay for the NACA 23012 section, equal to the gradient of the straight line fit, will be greater than that of the modified model.

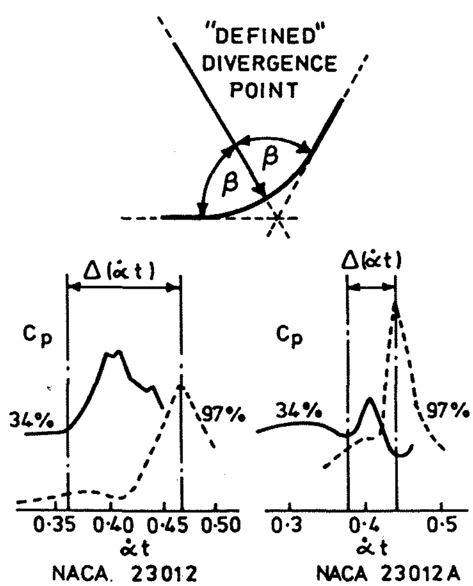

Fig. 10(a). DEFINED DIVERGENCE POINTS For individual pressure traces

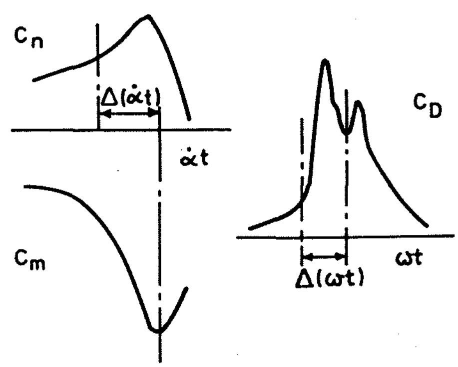

Fig. 10(b). DEFINED DIVERGENCE POINTS For integrated pressure traces

The important result, however, is that for both the ramp and the oscillatory cases, the time delay, is independent of either the reduced pitch rate or reduced frequency. The results for the oscillatory case, however, are confused by an apparent independence of non-dimensional time delay on mean angle of oscillation for the NACA 23012, and the evident dependence for the modified aerofoil. Even so, there are unmistakable good straight line correlations through the individual data sets as indicated in the legend and, for an explanation of these differences, we again consider the initial timing mark.

For the basic 23012 section, the "static" stalling characteristics (observed in the Glasgow facility[18]) are those of a very rapid movement of trailing edge separation at an incidence of 14.2°. The modified section was designed to retain the leading edge conditions of the unmodified aerofoil, over the first 25% of the chord, whilst enhancing the trailing edge separation at the lower angles of attack. This gave a more progressive and controlled penetration of trailing edge separation, towards the leading edge. The net apparent effect of this on the dynamic stall is, that for the NACA 23012, there was little difference in the location of the stall onset for both mean angles quoted. This is not the case for the modified version, where there were significant differences in separation front between the mean angles of 15 and 20°. This may indicate that the method of assessing time delays in the present work, is too simple an approach, albeit the difference between the respective time delays is small.

It is reasonable to conclude, therefore, that the development of the stall, once initiated, is independent of the type of the model motion and the speed at which this occurs, even although some difficulty is encountered in defining a consistent initial timing mark. It is, therefore, soon after stall onset, that the type of flow effectively undergoes a transition from a streamlined body dependent on the model and model motion, to that of a bluff body with a predominant dependence on freestream velocity.

Within the limitations of the facility[14], a series of tests at constant reduced pitch rate was carried out for a range of Reynolds numbers. Unfortunately, the discriminators used for fig. 9 deteriorated in quality due to the increased signal to noise ratio, as the Reynolds number was lowered. The various events associated with the stall manifest themselves through the aerodynamic coefficients, and these were used for timing purposes. The procedure used is shown in fig. 10a which illustrates the $\Delta(\dot{\alpha}t)$ value between the lift diversion and the minimum pitching moment. Only data for ramp motions were collected and the result is presented in fig. 11. For a fixed reduced pitch rate, a constant time delay (τ_r), between the chosen events, will be represented by parallel lines. The corresponding data, particularly between C_N divergence and C_M(min) are reasonably parallel and so favour the existence of a constant time delay.

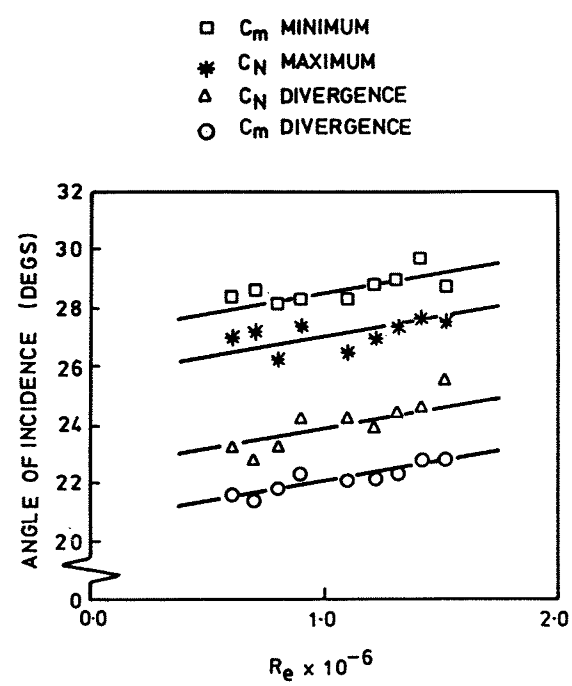

Fig. 11. VARIATION OF FORCE AND MOMENT CHARACTERISTICS WITH REYNOLDS NUMBER.

III. Other Aerofoils

If the observations from the Glasgow data are valid, and that the dynamic stall process becomes flow dependent soon after stall onset, then similar results should be obtainable from alternative data sources. Several data sets from ref. 7, which exhibit deep dynamic stall in comparable conditions to the above, have been analysed. For these data, however, the relevant duration of the stall was taken from the given drag history, as illustrated in fig. 10b. This particular method gave well defined descriminators and fig. 12 illustrates the results obtained. It is clear, that for the three aerofoils considered, there is a reasonable straight line correlation and comparability with the results presented in fig. 9. This comparability may be judged from tab. 2 which is a summary of the above correlations and that of other authors.

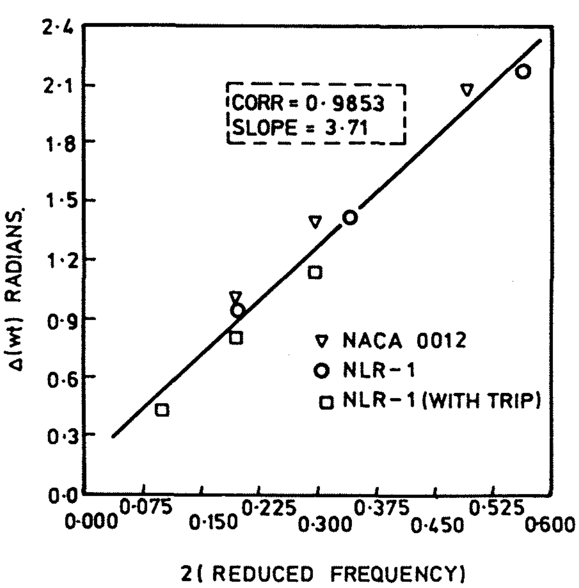

Fig.12. DRAG ANALYSIS - SINUSOIDAL TESTS (From Ref. 7)

DATA SOURCE	ANALYSIS TYPE	τ	CORR.
NACA 23012 OSCILLATORY 15±10	C_p at 34% and 97%	3.63	0·9959
NACA 23012A OSCILLATORY 15±10	" "	3·53	0·9992
20±10	" "	4·02	0·9986
NACA 23012 RAMP	" "	3·94	0·9938
NACA 23012A RAMP	" "	3·77	0·9951
NASA DATA (Ref.7)	C_D PLOT (FIG.12)	3·71	0·9853
BEDDOES (Ref.8)	C_p PLOT (FIG.5)	3·80	—
CARTA (Ref.9)	CONTOURS (FIG.2)	2·38 ← † ← 6·19	—

TABLE 2. TIME DELAY SUMMARY

† Calculated from wave velocities

IV. Conclusions

The data presented favours the hypothesis of the dynamic stall development, once initiated, being predominantly mean flow dependent rather than on the model motion etc. As a consequence of this, it follows that there are constant non-dimensional time delays associated with the process and that the normalised pressure wave velocity, over the upper surface of the aerofoil, is constant and independent of parameters such as reduced frequency etc.

The reconciliation of these conclusions with those of an alternative hypothesis (sect. 1) would require a more detailed and comprehensive assessment of the differences between the various facilities, measurement procedures and data analysis.

Acknowledgements

The authors wish to acknowledge the encouragement and support of Professor B.E. Richards and their colleagues both academic and technical.

The work was carried out in collaboration with Westland Helicopters via an SERC CASE award 8051/3408 and the RAE under MOD Agreement No. 2048/026XR/STR.

References

1. McCroskey, W.J. The Phenomenon of Dynamic Stall. Lecture Series 1981-84 in Unsteady Airloads and Aeroelastic Problems in Separated and Transonic Flow. Von Karman Institute for Fluid Dynamics, March 1981.

2. Beddoes, T.S. Short Course in Unsteady Aerodynamics (Rotor Applications). Von Karman Institute, March 1980.

3. Philippe, J.J. Dynamic Stall: An Example of Strong Interaction between Viscous and Inviscid Flows. AGARD CP-227, 1977.

4. Galbraith, R.A.McD. and Vezza, M. Methods of Predicting Dynamic Stall. Eighth BWEA Wind Energy Conference, Cambridge, 1986.

5. McCroskey, W.J. Recent Developments in Rotor Blade Stall. US Army Air Mobility ReD Laboratory, Ames Directorate, Moffett Field, California, USA, 94035.

6. Young, W.H. Jr. Fluid Mechanics Mechanism in the Stall Process for Helicopters. USAAVRADCOM TR 81-B-1, NASA TM 81956, 1981.

7. McCroskey, W.J., McAlister, K.W., Carr, L.W. and Pucci, S.L. An Experimental Study of Dynamic Stall on Advanced Airfoil Sections, Vol. 1, 2, 3. NASA TM 84245, 1982.

8. Beddoes, T.S. A Qualitative Discussion of Dynamic Stall. Aeromechanics Dept., Westland Helicopters, Yeovil, Somerset, BA20 2YB.

9. Carta, F.O. Analysis of Oscillatory Pressure Data including Dynamic Stall Effects. NASA CR-2394, May 1974.

10. Robinson, M.C. and Luttges, M.W. Unsteady Flow Separation and Attachment Induced by Pitching Airfoils. AIAA-83-0131, January, 1983.

11. Aihara, Y, Koyama, H. and Murashige, A. Transient Aerodynamic Characteristics of a Two-Dimensional Airfoil during Stepwise Incidence Variation. University of Tokyo, September 1984.

12. Beddoes, T.S. A Synthesis of Unsteady Aeordynamic Effects including Stall Hysteresis. Westland Helicopters Ltd.

13. Seto, L.Y. and Galbraith, R.A.McD. The Effect of Pitch Rate on the Dynamic Stall of a NACA 23012 Aerofoil. Paper No. 34, Eleventh European Rotorcraft Forum, September 1985.

14. Galbraith, R.A.McD. and Leishman, J.G. A Microcomputer Based Test Facility for the Investigation of Dynamic Stall. Paper E3, International Conference on the Use of the Micro in Fluid Engineering, 1983.

15. Galbraith, R.A.McD. A Data Acquisition System for the Investigation of Dynamic Stall. Proc. of 2nd Int. Con. on Computational Methods and Experimental Measurement. Computational Mechanics Centre Publication, Southampton, 1984.

16. Seto, L.Y. and Galbraith, R.A.McD. The Collected Data for Ramp Function Tests on a NACA 23012 Aerofoil. Vol. 1: Description and Pressure Data. GU Aero. Report 8413, November 1984.

17. Leishman, J.G., Seto, L.Y. and Galbraith, R.A.McD. Collected Data for Oscillatory Pitch Tests on a NACA 23012 Aerofoil. Vols. 1 and 2. GU Aero. Report 8600, March 1986.

18. Seto, L.Y., Leishman, J.G. and Galbraith, R.A.McD. An Investigation of Three-Dimensional Stall Developments on NACA 23012 and NACA 0012 Aerofoils. GU Aero. Report 8300, October 1984.